LETTERS

The purpose of this Letters section is to provide rapid dissemination of important new results in the fields regularly covered by Physics of Plasmas. Results of extended research should not be presented as a series of letters in place of comprehensive articles. Letters cannot exceed three printed pages in length, including space allowed for title, figures, tables, references and an abstract limited to about 100 words. ***There is a three-month time limit, from date of receipt to acceptance, for processing Letter manuscripts. Authors must also submit a brief statement justifying rapid publication in the Letters section.***

Dynamo action in the Taylor–Green vortex near threshold

C. Nore[a)] and M. E. Brachet
Laboratoire de Physique Statistique, CNRS URA 1306, ENS Ulm, 24 Rue Lhomond, 75231 Paris Cedex 05, France

H. Politano and A. Pouquet
Observatoire de la Côte d'Azur, CNRS URA 1362, BP 229, 06304 Nice-Cedex 4, France

(Received 17 April 1996; accepted 10 October 1996)

Dynamo action is demonstrated numerically in the forced Taylor–Green (TG) vortex made up of a confined swirling flow composed of a shear layer between two counter-rotating eddies, corresponding to a standard experimental setup in the study of turbulence. The critical magnetic Reynolds number above which the dynamo sets in depends crucially on the fundamental symmetries of the TG vortex. These symmetries can be broken by introducing a scale separation in the flow, or by letting develop a small non-symmetric perturbation which can be either kinetic and magnetic, or only magnetic. The nature of the boundary conditions for the magnetic field (either conducting or insulating) is essential in selecting the fastest growing mode; implications of these results to a planned laboratory experiment are briefly discussed. © *1997 American Institute of Physics.* [S1070-664X(97)02501-9]

The primary objective of this Letter is to demonstrate that a forced Taylor–Green vortex is consistent with a long term magnetic field produced by dynamo action and to find the critical magnetic Reynolds number for the field to be produced. The Taylor–Green (TG) vortex is a standard turbulent flow used in numerical computations[1,2] that is related to an experimentally studied swirling flow.[3–5] The relation between the experimental flow and the TG vortex is a similarity in overall geometry:[3] a shear layer between two counter-rotating eddies. The TG vortex, however, is periodic with free-slip boundaries while the experimental flow is contained inside a tank between two counter-rotating disks. One experiment in Gallium is planned,[6] in which the magnetic Reynolds number may be close to the critical value R_c^m above which a dynamo sets in.

The magnetohydrodynamics (MHD) equations for incompressible fluids with $\nabla\cdot\mathbf{v}=0$ and $\nabla\cdot\mathbf{b}=0$ read as

$$\partial_t\mathbf{v}+\mathbf{v}\cdot\nabla\mathbf{v}=-\rho_0^{-1}\nabla P+\nu\nabla^2\mathbf{v}+\mathbf{j}\times\mathbf{b}+\mathbf{F}(t), \tag{1}$$

$$\partial_t\mathbf{b}=\mathrm{curl}(\mathbf{v}\times\mathbf{b})+\eta\nabla^2\mathbf{b}, \tag{2}$$

where $\mathbf{b}$ is the Alfvén velocity $\mathbf{B}/\sqrt{4\pi\rho_0}$, ρ_0 the constant density, ν the kinematic viscosity, η the magnetic diffusivity and P the pressure; finally, $\mathbf{j}=\nabla\times\mathbf{b}$ is the current density. The governing parameter for the dynamo is the magnetic Reynolds number defined as $R^m=V_0L_{int}/\eta$, where V_0 is the rms velocity and L_{int} the integral scale, with $P^m=\nu/\eta$ the magnetic Prandtl number. An external driving volumic force $\mathbf{F}(t)$ is introduced in order to balance the energy dissipation and reach a statistically steady state; it is chosen as $\mathbf{F}(t)=f(t)\mathbf{v}^{TG}$, where $f(t)$ is determined by imposing that the (k_0,k_0,k_0) Fourier mode of $\mathbf{v}$ is fixed at all times to its initial value $\mathbf{v}^{TG}=(\sin(k_0x)\cos(k_0y)\cos(k_0z),-\cos(k_0x)\times\sin(k_0y)\cos(k_0z),0)$. A number of symmetries of $\mathbf{v}^{TG}$ are dynamically compatible with the equations of motion,[1] i.e., if the initial data obeys the same symmetries than $\mathbf{v}^{TG}$, then the solution, $\mathbf{v}_s$, is also symmetric. The symmetries of $\mathbf{v}_s$ amount,[1] with $k_0=1$, to the expansion $\mathbf{v}_s=\Sigma_{m,n,p}(\hat{u}_{sx}\times(m,n,p,t)\sin mx\cos ny\cos pz,\ \hat{u}_{sy}(m,n,p,t)\cos mx\sin ny\times\cos pz,\ \hat{u}_{sz}(m,n,p,t)\cos mx\cos ny\sin pz)$ where $\hat{\mathbf{u}}_s(m,n,p,t)$ vanishes unless m,n,p are either all even or all odd integers. The expansion coefficients obey the additional relations: $\hat{u}_{sx}^{(r)}(m,n,p)=(-1)^{r+1}\hat{u}_{sy}^{(r)}(n,m,p)$ and $\hat{u}_{sz}^{(r)}\times(m,n,p)=(-1)^{r+1}\hat{u}_{sz}^{(r)}(n,m,p)$, where $r=1$ when m,n,p are all even and $r=2$ when m,n,p are all odd. The corresponding symmetries of $\mathbf{v}_s$ in physical space are rotational symmetries: of angle π around the axis $(x=z=\pi/2)$ and $(y=z=\pi/2)$; and of angle $\pi/2$ around the axis $(x=y=\pi/2)$. There are also planes of mirror symmetry: $x=0,\pi$, $y=0,\pi$, $z=0,\pi$. The velocity and the vorticity $\boldsymbol{\omega}_s=\nabla\times\mathbf{v}_s$ are, respectively, parallel and perpendicular to these planes that form the sides of the so-called *impermeable box* which confines the flow. The kinetic helicity $h_s(\mathbf{x})=\mathbf{v}_s\cdot\boldsymbol{\omega}_s$ is *anti-symmetric* with respect to the planes of mirror symmetries. Thus, the total helicity of the TG flow $\langle h_s(\mathbf{x})\rangle\equiv0$ when integrated over the whole periodicity box $x=0,2\pi$, $y=0,2\pi$, $z=0,2\pi$. However, locally the helicity is strong: the eddy at the top of the impermeable box entrains an aspirating motion upward with velocity and vorticity antiparallel, and similarly for the counter-rotating eddy at the

bottom of the box.[1] Likewise, the spectrum of helicity $H_s^v(\mathbf{k})$ is non-zero, but the isotropic spectrum (when integrated over all angles) is again zero. Note that, because helicity provides an efficient mechanism for growth of the large-scale magnetic field,[7] ABC flows which are Beltrami ($\mathbf{u}=\pm\boldsymbol{\omega}/k_0$) are obvious candidates for dynamo action.[8,9] A dynamo in a highly symmetric flow with $\langle h(\mathbf{x})\rangle\equiv 0$ has been demonstrated numerically[10] using a hyperviscosity algorithm whereby the two diffusive operators in (1), (2) are replaced by higher powers of the Laplacian. Here, the choice is made to deal with the primitive MHD equations instead.

However, the above TG symmetries of $\mathbf{v}_s$ can physically be *spontaneously broken*, in the sense that a small non-symmetric component of the initial data will grow and eventually completely break the symmetry of the solution. Thus, in order to take this possibility into account, two periodic (with periodicity length $\mathscr{L}=2\pi$) pseudo-spectral codes are used. Both are de-aliased by the 2/3 rule. The wavenumbers are thus integers in the range ($k_{min}=1, k_{max}=N/3$), where N^3 is the number of grid points. The first code is a standard periodic code in which no symmetries are implemented. The second code is symmetric. It is used to save computer resources: implementing the TG symmetries yields, compared to the same computation in a general periodic code, a saving by a factor of 64 in both CPU and memory.[1] At a given Reynolds number $R^v=V_0L_{int}/\nu$, this represents, at equal cost, an increase of $64^{1/4}\sim 3$ in Reynolds number. The symmetric code was developed from the hydrodynamical version described in Ref. 1. All the symmetries of $\mathbf{v}_s$ (with $k_0=1$) are implemented within this code. Thus, no flow can cross the impermeable box $x=0,\pi$, $y=0,\pi$, $z=0,\pi$. The magnetic field in the symmetric code was chosen to have the same symmetries than $\mathbf{v}_s$, which can readily be checked to be dynamically compatible with the governing equation (2). Thus, $\mathbf{j}$ is perpendicular to the sides of the impermeable box.

In order to study linear growth-rates as a function of magnetic Reynolds number, both the general periodic and the symmetric code are initialized in a similar way. The initial velocity field is such that the kinetic energy corresponds to its (statistically) stationary value under the action of the TG forcing; and the magnetic field is initially set to a small seed value, such that $\beta_0=\langle\mathbf{b}^2\rangle/\langle\mathbf{v}^2\rangle\ll 1$. After initial transients die out, the growth–rates computed on $\langle\mathbf{a}^2\rangle$ (where $\mathbf{b}=\boldsymbol{\nabla}\times\mathbf{a}$), $\langle\mathbf{b}^2\rangle$ and $\langle\mathbf{j}^2\rangle$ are identical, corresponding to different Fourier projections of the same eigenmode. Two precautions have been taken when computing the growth-rates: (i) the linear character of the regime has been checked by decreasing β_0 (non-linear effects become noticeable when $\beta_0\simeq 10^{-4}$); (ii) the precision of the computation is measured by the logarithmic decrement $\delta(t)$ defined from a fit of energy spectra in the near dissipative range as $E(k,t)\sim\exp(-2\delta(t)k)$. It is such that for all times $\delta(t)k_{max}\sim 2$, a standard condition for computations of turbulent flows.[11] A symmetric run of $\sim 300\tau_{NL}$, where $\tau_{NL}=L_{int}/V_0\sim 0.6$ is the turn-over time, takes 4350 seconds of Cray $C94$ at a resolution of $N^3=128^3$.

The results of a series of computations at resolutions of 64^3, 128^3 and 200^3 points, corresponding to a wide range of magnetic Reynolds numbers R^m are summarized in Figure 1

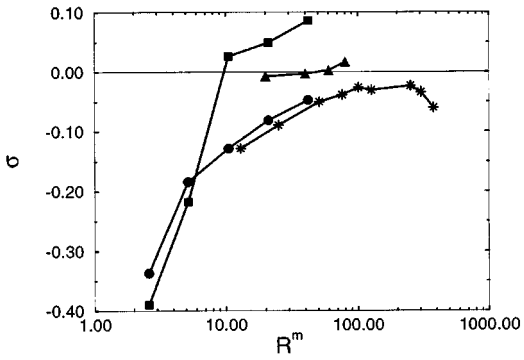

FIG. 1. Growth-rates σ of the square magnetic current as a function of $\log R^m$. Symbols for each computation differ according to the type of run: symmetric TG runs with $k_0=1$ and $R^v=51$ are represented by stars; symmetric TG runs with $k_0=1$ and $R^v=14.3$ by circles; symmetric TG runs with $k_0=2$ and $R^v=40$ by triangles, and squares are for the non-symmetric runs with $k_0=1$ and $R^v=14.3$ (see the text). Growth-rates for $\langle\mathbf{b}^2\rangle$ and $\langle\mathbf{a}^2\rangle$ are identical to those displayed here. Note that growing solutions only occur either when $k_0=2$ or for non-symmetric flows.

giving the growth-rate σ of the dynamo field as a function of R^m, with $\langle\mathbf{j}^2(t)\rangle\sim e^{\sigma t}$. Three types of runs are performed here: in the first case, symmetric TG runs with $k_0=1$ and $R^v=51$ (represented by stars) or with $k_0=1$ and $R^v=14.3$ (circles); in the second case, symmetric TG runs with $k_0=2$ and $R^v=40$ (triangles); finally, in the third case, runs using the general periodic code with $k_0=1$ and $R^v=14.3$ (squares). A simple test of the dynamical constraints imposed by the symmetries of the TG flow at $k_0=1$ is performed by comparing the results of the symmetric and general periodic runs at $R^v=14.3$. Initial conditions for these runs are identical except that, in the general periodic code, a non TG-symmetric perturbation of 1% in energy compared to that of the basic TG flow is introduced—at $t=0$ only—in the Fourier shell corresponding to $k=k_0$; both runs are at resolution $N=64$. In the non-symmetric runs (represented by squares), the resulting velocity settles at a larger kinetic energy than that at which the symmetric TG flow settles, namely $E^v\sim 0.28$ instead of 0.17; moreover, the total amount of kinetic helicity is non-zero; as measured by its relative rate $\rho^v=\langle\mathbf{v}\cdot\boldsymbol{\omega}\rangle/\sqrt{\langle\mathbf{v}^2\rangle\langle\boldsymbol{\omega}^2\rangle}$, we have $\rho^v\sim 5\%$. Thus, in the general periodic run, the TG symmetry is *spontaneously broken*, in the sense that the small initial non-TG-symmetric perturbation has changed the general character of the flow. As seen in Figure 1, the growth-rate remains negative in the symmetric case with $k_0=1$ (circles), whereas $R_c^m\sim 10$ in the general periodic case (squares).

Another result seen in Figure 1 is that, for the symmetric runs with $k_0=1$ and up to $R^m\sim 380$, growth-rates are always negative, whereas when taking $k_0=2$, one finds $\sigma\sim 0$ for $R_c^m\sim 50$. The drastic change of behavior obtained when $k_0=2$ may be due to a combination of two factors. First, when $k_0=2$, within the symmetry-conserving algorithm of a symmetric code, modes which are forbidden when $k_0=1$ can now be populated. For example, only modes with wavevector $(k_x=p,k_y=q,k_z=r)$, with (pqr) jointly even or odd, are present.[1] When $k_0=1$, both types of modes are generated from the initial data, whereas when $k_0=2$ only even modes are generated initially. Thus, in the $k_0=2$ case, there is a

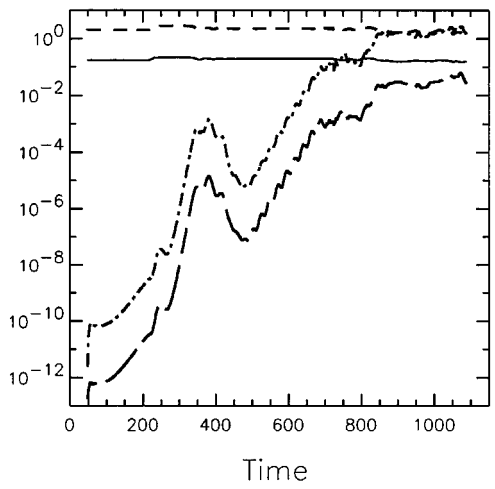

FIG. 2. Temporal evolution of the kinetic (solid line) and magnetic (long dash) energies as well as that of the square vorticity $\langle \boldsymbol{\omega}^2 \rangle$ (dash) and the square current $\langle \mathbf{j}^2 \rangle$ (dash–dot) for a run with $k_0=1$, $R^v=10.3$ and $R_m=41$, and with, at $t=0$, a pure TG velocity field. Note the substantially stronger growth in the secondary phase $270<Time<340$, followed by an oscillation and non-linear saturation.

possibility *within a symmetric TG code* for spontaneous symmetry breaking of the initial flow by the odd modes. A second factor is scale-separation: a similar effect was obtained in the study of the dynamo stirred by the ABC flow;[9] it was identified with the fact that the most unstable Fourier mode is at a scale slightly larger than that of the velocity. This is indeed the case in our symmetric computations where we find that the fastest growing mode has a Fourier component at wavenumber (1,1,1).

Whereas in the above non-symmetric runs, symmetries on both the velocity and the magnetic field have been initially broken, we now perform the more stringent test of using a non-symmetric magnetic seed with $\beta_0=10^{-12}$, but initially imposing all TG symmetries to the velocity, to within round-off errors. In that case, with $R^m=41$ and $R^v=10.3$, there is at first a weak growth of the magnetic field (recall that when **b** has the same symmetries as the TG flow, it does not grow at that Reynolds number). In Figure 2 are displayed the temporal evolution of the kinetic and magnetic energies, and $\langle \boldsymbol{\omega}^2 \rangle$ and $\langle \mathbf{j}^2 \rangle$ for that run. At $t\sim 220$, there is a spontaneous breaking of the TG symmetry of the velocity field, with an increase in kinetic energy which settles, after a transient, at $E^v=0.194$. This change in the velocity field allows for a substantial increase (roughly, a quadrupling) of the growth-rate of the magnetic energy. Non-linear effects are seen to become manifest for $\langle \mathbf{b}^2 \rangle / \langle \mathbf{v}^2 \rangle \sim 10^{-4}$ when an oscillation sets in, followed by a saturation at a level $\langle \mathbf{b}^2 \rangle \sim 8\times 10^{-2}$, whereas the ratio of maxima $b_{max}/v_{max} \sim 0.9$, indicative of an intermittent magnetic field. The details of the saturation regime are left for further studies. As for the non-symmetric growing runs of Figure 1, the growing non-symmetric magnetic field has Fourier components (0,0,1). Because of the relations $\boldsymbol{\nabla}\cdot\mathbf{b}=0$ and $\mathbf{j}=\boldsymbol{\nabla}\times\mathbf{b}$, the corresponding physical space fields have the form $\mathbf{b}=((a_x,a_y,0)\exp(iz)+\text{c.c.})$ and $\mathbf{j}=((-ia_x,ia_y,0)\exp(iz)+\text{c.c.})$, where c.c. denotes the complex conjugate. Thus, in a given horizontal cut $z=\text{const}$, both the magnetic field and the current are constant horizontal vector fields, perpendicular to each other. Such a *slab* geometry is forbidden in a symmetric TG code because of the invariance by rotation of angle $\pi/2$ around the axis $(x=y=\pi/2)$.

When comparing with an experimental setup, one has to take into account the fact that the magnetic Prandtl number of liquid metals is much smaller than unity, a regime unattainable with direct numerical simulations. However, a simple examination of the MHD equations setting $P^m \ll 1$ but keeping $R^m>1$ indicates that in the presence of an external large-scale magnetic field $\mathbf{B_0}$, an equilibrium in the induction equation is rapidly established, namely $\eta\Delta\mathbf{b}\sim\mathbf{B_0}\cdot\boldsymbol{\nabla}\mathbf{v}$; hence, in amplitude, $b\sim B_0 R^m$, similar to low thermal Prandtl number convection;[12] this suggests that a dynamo mechanism may work as well in the low P^m regime, granted R^m be sufficiently high.

Keeping this in mind, there are several implications of our results to experimental setups. First note that although $\langle h_s(\mathbf{x}) \rangle \equiv 0$, the kinetic helicity inside the impermeable box is strong. Experimentally, only the impermeable box is of relevance, and thus the experimental TG flow is strongly helical and likely a good candidate for dynamo action. Second, the present computations indicate that the regime of magnetic Reynolds numbers reachable experimentally may be close to criticality. Moreover, our results obtained with the general periodic code show that the fastest growing mode is a *slab mode* with **j** and **b** horizontal and perpendicular to each other. Thus, allowing for a magnetic field to loop outside the vessel in one horizontal direction, together with a large-scale current looping in the orthogonal direction, may significantly lower the critical magnetic Reynolds number for dynamo action to $R_c^m \simeq 10$. This type of circulation could be achieved experimentally by using materials with different conductibility at the wall, closing, outside the vessel, **j** with a conductor and **b** with a ferromagnetic material.

ACKNOWLEDGMENTS

Computations were performed on the C94–C98 of the Institut du Développement et des Ressources en Informatique Scientifique.

We received partial support from ''Mécanique des Fluides Géophysiques et Astrophysiques'' at the Centre National de la Recherche Scientifique, and from the European Cooperative Network ''Numerical Simulations of Nonlinear Magnetohydrodynamics'' (ERBCHRXCT930410).

[a]Electronic mail: nore@physique.ens.fr

[1] M. E. Brachet, D. I. Meiron, S. A. Orszag, B. G. Nickel, R. H. Morf, and U. Frisch, J. Fluid Mech. **130**, 411 (1983).
[2] M. E. Brachet, C. R. Acad. Sci. II **311**, 775 (1990).
[3] S. Douady, Y. Couder, and M. E. Brachet, Phys. Rev. Lett. **67**, 983 (1991).
[4] J. Maurer, P. Tabeling, and G. Zocchi, Europhys. Lett. **26**, 31 (1994).
[5] S. Fauve, C. Laroche, and B. Castaing, J. Phys. II France **3**, 271 (1993).
[6] S. Fauve (private communication, 1996).
[7] M. Steenbeck, F. Krause, and K-H Rädler, Z. Naturforsch. **21**, 369 (1966).
[8] D. Galloway and U. Frisch, Geophys. Astrophys. Fluid Dyn. **36**, 53 (1986).
[9] B. Galanti, P. L. Sulem, and A. Pouquet, Geophys. Astrophys. Fluid Dyn. **66**, 183 (1992).
[10] S. Kida, S. Yanase, and J. Mizushima, Phys. Fluids A **3**, 457 (1991).
[11] J. Jiménez, A. A. Wray, P. G. Saffman, and R. S. Rogallo, J. Fluid Mech. **255**, 65 (1993).
[12] K. Kumar, S. Fauve, and O. Thual, J. Phys. II **6**, 945 (1996).